Time-Domain Hydrodynamic Forces on Rigid Dams with Reservoir Bottom Absorption of Energy

Luis A. de Béjar, M.ASCE[1]

Abstract: In this investigation, a two-dimensional time-domain closed-form mathematical model for the hydrodynamic forces on the upstream vertical face of a given rigid dam subjected to a specified horizontal ground motion accelerogram was developed. The model includes the absorption of energy at the elastic reservoir bottom, characterized by the impedance ratio of the sub-bottom materials with respect to water (α). The formulated boundary-value problem is solved in Laplace's domain and subsequently transformed back to the time domain. Response spectra for the hydrodynamic base shear force and overturning moment are constructed for extreme values of the parameter α. It is found that, frequently, including the solid-foundation elasticity in the reservoir model attenuates the resultant hydrodynamic forces on a rigid barrier, as compared to the results for the case of a rigid reservoir foundation. In this case, the elasticity of the sub-bottom materials constitutes an effective energy dissipating mechanism (radiation damping). By contrast, for sub-bottom materials with less-than-water impedance, amplification of the effective earthquake forces is obtained, as compared to the results for the case of a rigid reservoir foundation.

DOI: 10.1061/(ASCE)EM.1943-7889.0000174

CE Database subject headings: Earthquakes; Hydrodynamics; Reservoirs; Absorption; Response spectra; Seismic analysis; Dams.

Author keywords: Earthquake; Hydrodynamic forces; Reservoir bottom absorption; Response spectra; Time-domain seismic analysis of dams.

Introduction

Realistic assessment of the response of dam-reservoir-foundation systems to earthquake excitation requires appropriate modeling of the sub-bottom absorption of energy. The acoustic impedance (or, equivalently, the coefficient of reflection) of the sub-bottom materials in relation to water has been found to adequately represent the corresponding equivalent damping in the boundary conditions of the governing equations of motion for the water medium in the frequency domain (Hall and Chopra 1982; Fenves and Chopra 1985b). However, the exact interaction of the reservoir with its foundation remains difficult to characterize.

When a water pressure wave traveling vertically downward strikes the bottom boundary surface, part of the propagating energy is reflected back into the reservoir and another part is transmitted to the foundation medium on account of its finite stiffness. Frequently, this refracted energy may be assumed to continue propagating vertically downward toward infinity, actually constituting an equivalent energy dissipating mechanism introducing radiation damping that effectively reduces the response of the system. On the other hand, if the sub-bottom materials contain large amounts of constituents with lower-than-water impedance, a substantial part of the incident pressure-wave energy may be reflected back into the reservoir as rarefaction waves, which in turn become reflected compression waves at the upper boundary surface (on air), which may reinforce the continuous input of pressure from the exciting dam motion. In other words, it is possible that the interaction of the reservoir with the sub-bottom materials effectively increases the magnitude of the system response (Cheng 1986; Bougacha and Tassoulas 1991). The resulting effect, as compared to the response for a rigid foundation, depends on both the actual impedance ratio of the foundation with respect to water and on the specific characteristics of the input ground motion acceleration, particularly on the content of large pulses.

This investigation presents a mathematical model to evaluate the force effect by the impounded water on retaining concrete gravity dams upon earthquake excitation, in the time domain, including the interaction of the reservoir with the sub-bottom materials. The time history of the hydrodynamic pressure field on the upstream face of the dam and the associated resultant lateral force and overturning moment are evaluated, allowing the construction of the corresponding response spectra for dam-reservoir-sub-bottom systems.

The analytical model is two dimensional (which is very appropriate for straight gravity dams) and the dam is considered as a rigid barrier. The reservoir is assumed infinitely long in the upstream direction. Water is assumed a homogeneous, inviscid, and linearly compressible fluid, and its flow is taken as irrotational. The boundary condition at the horizontal bottom of the reservoir is formulated accounting for the elasticity of the underlying medium. The sub-bottom is represented by means of a characteristic value of its impedance ratio with respect to water. The exciting input ground motion acceleration is assumed to be acting in the horizontal direction (parallel to the reservoir bottom) only and the initial conditions of the system are assumed to be at rest. Hydrostatic forces and the secondary effect of gravity waves are ignored.

The direct analysis in the time domain offers some definite

[1]Research Structural Engineer, U.S. Army Engineer Research and Development Center, Vicksburg, MS 39180-6199.

Note. This manuscript was submitted on February 9, 2010; approved on March 23, 2010; published online on March 25, 2010. Discussion period open until March 1, 2011; separate discussions must be submitted for individual papers. This paper is part of the ***Journal of Engineering Mechanics***, Vol. 136, No. 10, October 1, 2010. ©ASCE, ISSN 0733-9399/2010/10-1271–1280/$25.00.

Report Documentation Page

Form Approved
OMB No. 0704-0188

1. REPORT DATE	2. REPORT TYPE	3. DATES COVERED
OCT 2010		**00-00-2010 to 00-00-2010**

4. TITLE AND SUBTITLE	5a. CONTRACT NUMBER
Time-Domain Hydrodynamic Forces On Rigid Dams With Reservoir Bottom Absorption Of Energy	5b. GRANT NUMBER
	5c. PROGRAM ELEMENT NUMBER
6. AUTHOR(S)	5d. PROJECT NUMBER
	5e. TASK NUMBER
	5f. WORK UNIT NUMBER
7. PERFORMING ORGANIZATION NAME(S) AND ADDRESS(ES) **U.S. Army Engineer Research and Development Center,Vicksburg,MS,39180**	8. PERFORMING ORGANIZATION REPORT NUMBER
9. SPONSORING/MONITORING AGENCY NAME(S) AND ADDRESS(ES)	10. SPONSOR/MONITOR'S ACRONYM(S)
	11. SPONSOR/MONITOR'S REPORT NUMBER(S)

12. DISTRIBUTION/AVAILABILITY STATEMENT
Approved for public release; distribution unlimited

13. SUPPLEMENTARY NOTES
Journal Of Engineering Mechanics, October 2010, pgs 121-180

14. ABSTRACT

In this investigation, a two-dimensional time-domain closed-form mathematical model for the hydrodynamic forces on the upstream vertical face of a given rigid dam subjected to a specified horizontal ground motion accelerogram was developed. The model includes the absorption of energy at the elastic reservoir bottom, characterized by the impedance ratio of the sub-bottom materials with respect to water . The formulated boundary-value problem is solved in Laplace?s domain and subsequently transformed back to the time domain. Response spectra for the hydrodynamic base shear force and overturning moment are constructed for extreme values of the parameter . It is found that, frequently, including the solid-foundation elasticity in the reservoir model attenuates the resultant hydrodynamic forces on a rigid barrier, as compared to the results for the case of a rigid reservoir foundation. In this case, the elasticity of the sub-bottom materials constitutes an effective energy dissipating mechanism radiation damping . By contrast, for sub-bottom materials with less-than-water impedance, amplification of the effective earthquake forces is obtained, as compared to the results for the case of a rigid reservoir foundation.

15. SUBJECT TERMS

16. SECURITY CLASSIFICATION OF:			17. LIMITATION OF ABSTRACT	18. NUMBER OF PAGES	19a. NAME OF RESPONSIBLE PERSON
a. REPORT **unclassified**	b. ABSTRACT **unclassified**	c. THIS PAGE **unclassified**	**Same as Report (SAR)**	**11**	

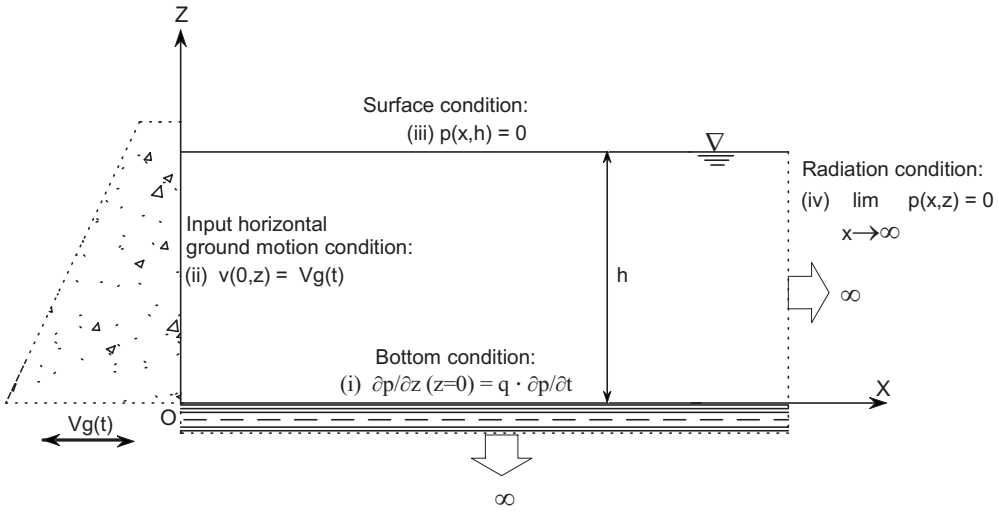

Fig. 1. Two-dimensional analytical model for a rigid dam, the impounded water, and the reservoir bottom

advantages over the alternative conventional techniques in the frequency domain. First, the resulting models can easily be extended to represent the behavior of flexible dams exhibiting material nonlinearities. Nonlinear frequency-domain analysis, even when possible at all, is extremely cumbersome. Second, analysis in the time domain is agreeable to the intuition of engineers. In fact, direct time-domain analysis using a closed-form solution allows practical and efficient assessment of the hydrodynamic forces on barriers in reservoir-dam systems subjected to general earthquake excitations (much of the seismic frequency-domain researches in dam engineering to date have been limited to harmonic earthquakes (Bouaanani et al. 2003; Fenves and Chopra 1985a; Gogoi and Maity 2006). The corresponding numerical analyses in the frequency domain are more intricate, involving the use of fast-Fourier-transform algorithms (Fenves and Chopra 1983, 1984a,b). Finally, but most important, the simple closed-form solution in the time domain allows expedient and realistic assessment of the frequent economical advantages of including bottom absorption in the engineering estimation of earthquake hydrodynamic forces on dams, including the efficient generation of response spectra, for a given site and design ground motion. Previous investigations in the time domain invariably implement numerical methods of solution (Weber 1994).

Mathematical Models

Problem Formulation

The physical behavior of the dam-reservoir-sub-bottom system is described mathematically by the two-dimensional wave equation in terms of the velocity potential for the water particles in the reservoir, ϕ (Kotsubo 1959)

$$\nabla^2\phi - \frac{1}{c^2}\cdot\frac{\partial^2}{\partial t^2}\phi = 0 \tag{1}$$

where ∇^2=Laplacian operator $\partial^2/\partial x^2+\partial^2/\partial z^2$ and c=velocity of propagation of the pressure waves in the water.

Fig. 1 shows schematically the boundary conditions at the four edges of the water domain, identified as (i)–(iv). Boundary condition (i) refers to the bottom of the reservoir and represents the absence of the vertical component of acceleration for the water particles in contact with the solid bottom material since the input ground motion is assumed to act exclusively in the horizontal direction.

In the frequency domain, the gradient of the Fourier transform of the pressure field in the direction of the local normal to the contact surface at the bottom consists of two distinct terms. One term due to the free-field ground acceleration at the site, with local normal component a_n, and another term due to the static interaction between the solid and the fluid media upon reflection and refraction of the pressure waves at the interface between these two phases owing to their different elastic properties (Rosenblueth 1968; Hall and Chopra 1982). The corresponding relationship may be expressed mathematically as

$$\frac{\partial \mathrm{P}(w)}{\partial n} = -\rho\cdot a_n + (iw)\cdot q\cdot \mathrm{P}(w) \tag{2a}$$

where P(w)=Fourier transform of the pressure field in the water; ρ=density of water; w=frequency-domain variable; i= imaginary unit; and q is given by

$$q = \frac{\rho}{\rho_r\cdot c_r} \tag{2b}$$

in which ρ_r=density of the sub-bottom material and c_r=velocity of propagation of the pressure waves through the same medium, i.e., the product $(q\cdot c)$ is the impedance ratio of water with respect to the foundation material. Alternately, the product $(q\cdot c)$ may also be expressed in terms of the coefficient of reflection of the sub-bottom material with respect to water (β_r), defined for the pure-interaction problem (i.e., when there is no free-field ground motion acceleration), as

$$q\cdot c = \frac{1-\beta_r}{1+\beta_r} = \frac{1}{\alpha} \tag{2c}$$

where α=impedance ratio of the sub-bottom material with respect to water, i.e.

$$\alpha = \frac{\rho_r\cdot c_r}{\rho\cdot c} \tag{2d}$$

Since the vertical component of ground motion acceleration (a_n) is zero in the problem being formulated, boundary condition (i), expressed by Eq. (2a) in the frequency domain, reduces to

$$\frac{\partial \mathrm{P}(w)}{\partial n} = (iw) \cdot q \cdot \mathrm{P}(w) \tag{3a}$$

which may be written in the time domain as

$$\frac{\partial p}{\partial n} - q \cdot \frac{\partial p}{\partial t} = \frac{\partial p}{\partial z} - q \cdot \frac{\partial p}{\partial t} = 0, \quad \text{at} \quad z = 0 \tag{3b}$$

where $p(x,z,t)$=hydrodynamic pressure field, given by (Newmark and Rosenblueth 1971)

$$p(x,z,t) = \rho \cdot \frac{\partial \phi}{\partial t} \tag{4}$$

Therefore, boundary condition (i) in the time domain becomes

$$\left(\frac{\partial \phi}{\partial z}\right)\bigg|_{z=0} = q \cdot \frac{\partial \phi}{\partial t} \tag{5}$$

Eq. (5) is the distinctive boundary condition for the time domain analysis of a dam-reservoir-flexible-subbottom system subjected to earthquake excitation. The other three boundary conditions remain the same as for the associated rigid foundation problem (Kotsubo 1959), i.e.,

(ii) The horizontal velocity of the water particles in direct contact with the upstream face of the dam is given by the function for the ground motion velocity. This is expressed mathematically as

$$-\frac{\partial \phi}{\partial x}\bigg|_{x=0} = V_g(t) \tag{6}$$

(iii) The hydrodynamic pressure at the upper edge of the water domain is zero (ignoring the effect of gravity waves). Or, expressed mathematically, in terms of the water velocity potential, one has

$$\frac{\partial \phi}{\partial t}\bigg|_{z=h} = 0 \tag{7}$$

(iv) Very far away from the direct disturbance of the water medium, all hydrodynamic responses of the water should tend asymptotically to zero (radiation condition). This is expressed mathematically as

$$\lim_{x \to \infty} \phi = 0 \tag{8}$$

To complete the formulation of the problem in the time domain, in addition to these boundary conditions, zero initial conditions are assumed for the system, i.e., in terms of the water velocity potential, one has

$$\phi(0) = \text{const} \ (=0) \tag{9a}$$

and

$$\frac{\partial \phi}{\partial t}(0) = 0 \tag{9b}$$

Laplace Transformation of the Problem

Taking the Laplace transformation of the wave Eq. (1) with respect to time, the governing differential equation becomes the following Helmholtz equation

$$\nabla^2 \Phi - \frac{s^2}{c^2} \cdot \Phi = 0 \tag{10}$$

where $\Phi = \mathrm{T}(\varphi)$=Laplace transformation of the water velocity potential, and s is the basic variable in Laplace's domain. Boundary conditions (i)–(iv) may also be correspondingly transformed to give

$$\frac{\partial \Phi}{\partial z}\bigg|_{z=0} = q \cdot s \cdot (\Phi)|_{z=0} \tag{11a}$$

$$-\frac{\partial \Phi}{\partial x}\bigg|_{x=0} = \mathrm{T}[V_g(t)] \tag{11b}$$

$$\Phi|_{z=h} = 0 \tag{11c}$$

and

$$\lim_{x \to \infty} \Phi = 0 \tag{11d}$$

Problem Transformation within Laplace's Domain

Looking for homogeneous boundary conditions with respect to the independent variable z, let the transform of the unknown velocity potential be defined in terms of a new field in Laplace's domain, Ψ, according to

$$\Phi = e^{-q \cdot s \cdot (h-z)} \cdot \Psi \tag{12}$$

When Eq. (12) is substituted in Eq. (10), the new governing differential equation is obtained as

$$\nabla^2 \Psi + 2 \cdot q \cdot s \cdot \frac{\partial \Psi}{\partial z} + (q \cdot s)^2 \cdot \left(1 - \frac{1}{(q \cdot c)^2}\right) \cdot \Psi = 0 \tag{13}$$

and the boundary conditions expressed by Eqs. (11*a*) and (11*c*) become

$$\frac{\partial \Psi}{\partial z}\bigg|_{z=0} = 0 \tag{14a}$$

and

$$\Psi|_{z=h} = 0 \tag{14b}$$

respectively.

Problem Solution in Laplace's Domain

This boundary-value problem is conveniently solved for the field Ψ in Laplace's s-domain by separation of variables. By assuming $\Psi = X(x,s) \cdot Z(z,s)$, Eq. (13) may be written as (Wylie 1975)

$$\left(\frac{X''}{X} - \frac{s^2}{c^2}\right) + \left(\frac{Z''}{Z} + 2 \cdot q \cdot s \cdot \frac{Z'}{Z} + q^2 \cdot s^2\right) = 0 \tag{15}$$

where $Z' = \partial Z / \partial z$, $Z'' = \partial^2 Z / \partial z^2$, and $X'' = \partial^2 X / \partial x^2$. One way to satisfy Eq. (15) is by having the first parenthesis in this equation equal to a positive constant λ^2, while the second parenthesis in the equation equal to the negative of the same constant, i.e.

$$\frac{X''}{X} - \frac{s^2}{c^2} = \lambda^2 \tag{16a}$$

and

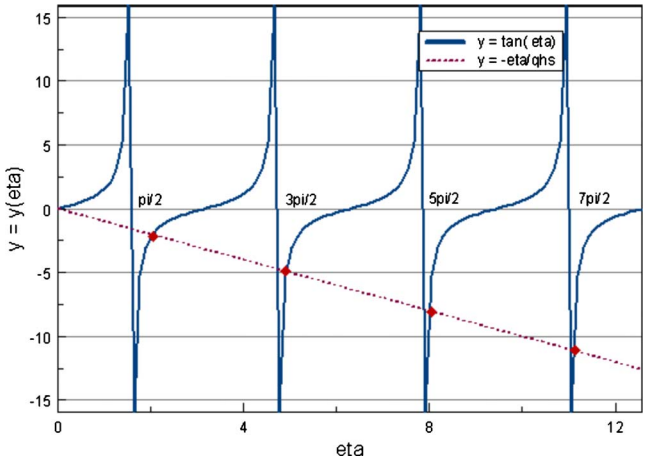

Fig. 2. Graphical representation of the numerical solution for the eigenproblem formulated in Eq. (20)

$$\frac{Z''}{Z} + 2 \cdot q \cdot s \cdot \frac{Z'}{Z} + q^2 \cdot s^2 = -\lambda^2 \tag{16b}$$

The general solution of Eq. (16*b*) is

$$Z(z,s) = e^{-q \cdot s \cdot z} \cdot [A(s) \cdot \cos(\lambda \cdot z) + B(s) \cdot \sin(\lambda \cdot z)] \tag{17}$$

Imposing boundary condition (14*a*) into Eq. (17) leads to the relation

$$-q \cdot s \cdot A(s) + \lambda \cdot B(s) = 0 \tag{18a}$$

while imposing boundary condition (14*b*) into Eq. (17) leads to the relation

$$A(s) \cdot \cos(\lambda \cdot h) + B(s) \cdot \sin(\lambda \cdot h) = 0 \tag{18b}$$

Putting Eqs. (18*a*) and (18*b*) into a single matrix equation gives the following eigenproblem:

$$\begin{bmatrix} -q \cdot s & \lambda \\ \cos(\lambda \cdot h) & \sin(\lambda \cdot h) \end{bmatrix} \cdot \begin{Bmatrix} A(s) \\ B(s) \end{Bmatrix} = \begin{Bmatrix} 0 \\ 0 \end{Bmatrix} \tag{19}$$

A necessary condition for this algebraic system of homogeneous equations to produce a nontrivial solution is that the determinant of the coefficient matrix be zero. Such condition leads to the following characteristic equation (which in this case is transcendental):

$$\tan \eta = -\frac{1}{q \cdot s \cdot h} \cdot \eta \tag{20}$$

where $\eta = \lambda \cdot h$. The solution of Eq. (20) yields an infinite number of eigenvalues, as indicated schematically in Fig. 2. The solid curves in the figure represent the left side of Eq. (20), whereas the dotted straight line represents the right side of the same equation. The abscissas of the points of intersection of the straight line with the set of curves (highlighted in the figure) are the solutions to Eq. (20), which must be determined numerically. In principle, these eigenvalues can be determined numerically with any desired level of accuracy. However, it is clear from the figure that, with the exception of the case in which s is "very large," after a few initial eigenvalues, the mth root of Eq. (20) is given approximately by

$$\eta_m = \lambda_m \cdot h \approx (2 \cdot m + 1) \cdot \frac{\pi}{2} \quad (m \geqslant 0) \tag{21}$$

independently of s. It will be subsequently shown that the contributions to the solution from very large values of s are negligible. Therefore, the eigenfunctions generated by Eq. (17) may be written as

$$Z_m(z,s) = A_m(s) \cdot e^{-q \cdot s \cdot z} \cdot \left(\cos(\lambda_m \cdot z) + \frac{q \cdot s}{\lambda_m} \cdot \sin(\lambda_m \cdot z) \right) \tag{22}$$

where λ_m is given by Eq. (21).

Now, Eq. (16*a*) renders the following ordinary differential equation:

$$X'' - \left(\lambda_m^2 + \frac{s^2}{c^2} \right) \cdot X = 0 \tag{23}$$

with general solution

$$X_m(x,s) = C_m(s) \cdot e^{-\sqrt{\lambda_m^2 + (s^2/c^2)} \cdot x} + D_m(s) \cdot e^{+\sqrt{\lambda_m^2 + (s^2/c^2)} \cdot x} \tag{24}$$

However, the second term in Eq. (24) diverges for very large values of the abscissa x. Consequently, on the basis of the radiation boundary condition expressed by Eq. (11*d*), we conclude that $D_m(s) = 0$.

Combining Eqs. (22) and (24) and letting $C_m(s)$ be absorbed by $A_m(s)$, one obtains the following eigenfunction associated with the eigenvalue λ_m:

$$\Psi_m(x,z,s) = A_m(s) \cdot e^{-q \cdot s \cdot z} \cdot \left(\cos(\lambda_m \cdot z) + \frac{q \cdot s}{\lambda_m} \cdot \sin(\lambda_m \cdot z) \right) \cdot e^{-\sqrt{\lambda_m^2 + (s^2/c^2)} \cdot x} \tag{25}$$

which is immediately transformed using the definition given by Eq. (12) as

$$\Phi_m(x,z,s) = e^{-q \cdot s \cdot (h-z)} \cdot \Psi_m(x,z,s) \tag{26}$$

Finally, the general solution field in Laplace's domain is the linear combination of the infinite number of eigenfunctions expressed by Eq. (26) to span the entire space of possible functions $\Phi(x,z,s)$, i.e.

$$\Phi(x,z,s) = e^{-q \cdot s \cdot h} \cdot \sum_{m=0}^{\infty} A_m(s) \cdot \left(\cos(\lambda_m \cdot z) + \frac{q \cdot s}{\lambda_m} \cdot \sin(\lambda_m \cdot z) \right) \cdot e^{-\sqrt{\lambda_m^2 + (s^2/c^2)} \cdot x} \tag{27}$$

To proceed any further, one needs to use the remaining boundary condition (11*b*) to evaluate the coefficients $A_m(s)$ for a specific input ground velocity.

Unit-Impulse Response Function

The unit-impulse response function represents the hydrodynamic-pressure response in the water when the input ground velocity is the Heaviside unit-step function at the initial time, or, equivalently, when the input ground acceleration is a Dirac delta function of unit intensity applied at the origin of time. Imposing boundary condition (11*b*) on Eq. (27), one obtains

$$\left.\frac{\partial \Phi}{\partial x}\right|_{x=0} = -e^{-q\cdot s\cdot h}\cdot \sum_{m=0}^{\infty} A_m(s)\cdot \sqrt{\lambda_m^2+\frac{s^2}{c^2}} \cdot\left(\cos(\lambda_m\cdot z)+\frac{q\cdot s}{\lambda_m}\cdot \sin(\lambda_m\cdot z)\right) = -\frac{1}{s} \quad (28)$$

where the last term in Eq. (28) is the Laplace transform of the negative of the Heaviside unit-step function at the initial time.

Any coefficient $A_i(s)$ is obtained by multiplying each side of Eq. (28) by $\cos(\lambda_i\cdot z)$, integrating with respect to the variable z within the domain $(-h,+h)$ and considering the known values of the following integrals:

$$\int_{-h}^{+h} \cos(\lambda_m\cdot z)\cdot\cos(\lambda_i\cdot z)dz = h\cdot\delta_{mi} \quad (29a)$$

$$\int_{-h}^{+h} \sin(\lambda_m\cdot z)\cdot\cos(\lambda_i\cdot z)dz = 0 \quad (29b)$$

and

$$\int_{-h}^{+h} \cos(\lambda_i\cdot z)dz = \frac{4h\cdot\sin\left((2\cdot i+1)\cdot\frac{\pi}{2}\right)}{(2\cdot i+1)\cdot\pi} = \frac{4h(-1)^i}{(2\cdot i+1)\cdot\pi} \quad (29c)$$

where δ_{mi}=Kronecker's delta. After some algebraic manipulations, the result is

$$A_i(s) = \frac{1}{\lambda_i\cdot h\cdot s}\cdot e^{q\cdot h\cdot s}\cdot\frac{2\sin(\lambda_i\cdot h)}{\sqrt{\lambda_i^2+\frac{s^2}{c^2}}} \quad (30)$$

Inserting Eq. (30), evaluated for $i=m$, into Eq. (27), the Laplace transform of the velocity potential is obtained as

$$\Phi(x,z,s) = \sum_{m=0}^{\infty}\frac{1}{\lambda_m\cdot h\cdot s}\cdot\frac{2\sin(\lambda_m\cdot h)}{\sqrt{\lambda_m^2+\frac{s^2}{c^2}}} \cdot\left(\cos(\lambda_m\cdot z)+\frac{q\cdot s}{\lambda_m}\cdot\sin(\lambda_m\cdot z)\right)\cdot e^{-\sqrt{\lambda_m^2+(s^2/c^2)}\cdot x} \quad (31)$$

Notice that this function goes to zero rapidly as s grows, confirming the earlier assertion that the region of very large values of s contributes negligibly to the response. Using Eq. (31), the unit-impulse response function $F(x,z,t)$ is obtained as

$$F(x,z,t) = \rho\cdot T^{-1}(s\cdot\Phi) = \rho\cdot\sum_{m=0}^{\infty}\frac{2\sin(\lambda_m\cdot h)}{\lambda_m\cdot h}\cdot\left\{\cos(\lambda_m\cdot z)\cdot T^{-1}\left(\frac{e^{-\sqrt{\lambda_m^2+(s^2/c^2)}\cdot x}}{\sqrt{\lambda_m^2+\frac{s^2}{c^2}}}\right) + \frac{q\cdot\sin(\lambda_m\cdot z)}{\lambda_m}\cdot T^{-1}\left(\frac{s\cdot e^{-\sqrt{\lambda_m^2+(s^2/c^2)}\cdot x}}{\sqrt{\lambda_m^2+\frac{s^2}{c^2}}}\right)\right\} \quad (32)$$

where $T^{-1}(\,)$=the inverse Laplace transform operator.

The first inverse Laplace transform in Eq. (32) is given by (Zwillinger 1996)

$$c\cdot T^{-1}\left[\frac{e^{-(x/c)\cdot\sqrt{(\lambda_m\cdot c)^2+s^2}\cdot}}{\sqrt{(\lambda_m\cdot c)^2+s^2}}\right] = c\cdot J_0[\lambda_m\cdot\sqrt{(c\cdot t)^2-x^2}],\quad c\cdot t>x \quad (33a)$$

The second inverse Laplace transform in Eq. (32) may be obtained using Eq. (33*a*) and the fact that

$$T\left[\frac{d\varphi(t)}{dt}\right] = s\cdot T[\varphi(t)]-\varphi(0^+) = s\cdot T[\varphi(t)] \quad (33b)$$

and therefore

$$T^{-1}\{s\cdot T[\varphi(t)]\} = \frac{d\varphi(t)}{dt} \quad (33c)$$

where $\varphi(t)$ is an arbitrary "well-behaved" function of the time t.

The complete Laplace inversion of Eq. (32) gives the unit-impulse response function as (Bowman 1958)

$$F(x,z,t) = 4\rho c\sum_{m=0}^{\infty}\frac{(-1)^m}{(2\cdot m+1)\cdot\pi}\cdot\left\{\cos(\lambda_m\cdot z)\cdot J_0[\lambda_m\cdot\sqrt{(c\cdot t)^2-x^2}] - \frac{c\cdot t}{\alpha}\cdot\frac{\sin(\lambda_m\cdot z)}{\sqrt{(c\cdot t)^2-x^2}}\cdot J_1[\lambda_m\cdot\sqrt{(c\cdot t)^2-x^2}]\right\},\quad c\cdot t>x \quad (34)$$

which simplifies considerably when evaluated on the upstream face of the dam ($x=0$) into

$$F^o(\zeta,t) = \frac{4\rho c}{\pi}\sum_{m=0}^{\infty}\frac{(-1)^m}{(2\cdot m+1)}\cdot\left\{\cos(\eta_m\cdot\zeta)\cdot J_0\left(\eta_m\cdot\frac{c\cdot t}{h}\right) - \frac{1}{\alpha}\cdot\sin(\eta_m\cdot\zeta)\cdot J_1\left(\eta_m\cdot\frac{c\cdot t}{h}\right)\right\}\cdot H(t) \quad (35a)$$

where $H(t)$=Heaviside unit-step function at the origin of time; J_i, $i=0,1,$ =Bessel function of the first kind and ith order; and $\zeta=z/h$=normalized ordinate of the point under consideration along the height of the dam face. Function $F^o(\zeta,t)$ reduces to the solution in the time domain previously reported by Kotsubo (1959) for a rigid foundation ($\alpha\to\infty$), i.e.

$$F^o(\zeta,t) = \frac{4\rho c}{\pi}\sum_{m=0}^{\infty}\frac{(-1)^m}{(2\cdot m+1)}\cdot\cos(\eta_m\cdot\zeta)\cdot J_0\left(\eta_m\cdot\frac{c\cdot t}{h}\right),\quad t>0 \quad (35b)$$

Solution for Input Ground Motion Accelerogram

The seismic hydrodynamic pressure field on the upstream face of the dam when the system is subjected to ground motion acceleration is readily computed from the convolution of the unit-impulse response function with the time history of the ground motion acceleration, $a_g(t)$ (Clough and Penzien 1993)

$$p^o(\zeta,t) = \int_0^t a_g(t-\tau)\cdot F^o(\zeta,\tau)d\tau = \gamma\cdot g\cdot\int_0^t \Gamma(t-\tau)\cdot F^o(\zeta,\tau)d\tau \tag{36}$$

where $p^0(\zeta,t)$=hydrodynamic pressure on the upstream face of the dam as a function of time; Γ=nondimensional input acceleration function; and $\gamma\cdot g$=peak ground motion acceleration, as a fraction (γ) of gravity (g).

Inserting Eq. (35*a*) into Eq. (36), one obtains the hydrodynamic-pressure response as

$$p^o(\zeta,t) = 4\cdot\frac{w_o\cdot c\cdot\gamma}{\pi}\cdot\sum_{m=0}^{\infty}\frac{(-1)^m}{(2\cdot m+1)}\cdot\left\{\cos(\eta_m\cdot\zeta)\cdot A_{0m}(t)-\frac{1}{\alpha}\cdot\sin(\eta_m\cdot\zeta)\cdot A_{1m}(t)\right\} \tag{37a}$$

where w_o=unit weight of water and

$$A_{im}(t) = \int_0^t \Gamma(t-\tau)\cdot J_i\left(\eta_m\cdot\frac{c\cdot\tau}{h}\right)d\tau,\quad i=0,1 \tag{37b}$$

Alternatively, Eq. (37*a*) may be normalized, for a nondimensional solution for the hydrodynamic pressure, as

$$\mathrm{T}^o(\zeta,t) = \frac{p^0(\zeta,t)}{w_0\cdot c\cdot\gamma} = \frac{4}{\pi}\cdot\sum_{m=0}^{\infty}\frac{(-1)^m}{(2\cdot m+1)}\cdot\left\{\cos(\eta_m\cdot\zeta)\cdot A_{0m}(t)-\frac{1}{\alpha}\cdot\sin(\eta_m\cdot\zeta)\cdot A_{1m}(t)\right\} \tag{38}$$

Resultant Hydrodynamic Force

The resultant earthquake hydrodynamic force on the upstream face of the dam $P^0(t)$ is obtained by integrating the pressure field along the height of the reservoir, i.e.

$$P^o(t) = h\cdot\int_0^1 p^o(\zeta,t)d\zeta \tag{39}$$

Inserting Eq. (37) into Eq. (39) and recognizing that

$$\int_0^1\cos(\eta_m\cdot\zeta)d\varsigma = \frac{(-1)^m}{\left(m+\frac{1}{2}\right)\cdot\pi} \tag{40a}$$

and

$$\int_0^1\sin(\eta_m\cdot\zeta)d\zeta \approx \frac{1}{\eta_m} \tag{40b}$$

the resultant hydrodynamic force is obtained as

$$P^o(t) = 8\cdot\frac{w_o\cdot c\cdot\gamma\cdot h}{\pi^2}\cdot\sum_{m=0}^{\infty}\frac{1}{(2\cdot m+1)^2}\cdot\left\{A_{0m}(t)-\frac{1}{\alpha}\cdot(-1)^m\cdot A_{1m}(t)\right\} \tag{41a}$$

or, normalizing, for a nondimensional solution, Eq. (41*a*) may be written as

$$\Omega_0 = \frac{P^o(t)}{w_o\cdot h^2} = \frac{32}{\pi^2}\cdot\gamma\cdot f\cdot\sum_{m=0}^{\infty}\frac{1}{(2\cdot m+1)^2}\cdot\left\{A_{0m}(t)-\frac{1}{\alpha}\cdot(-1)^m\cdot A_{1m}(t)\right\} \tag{41b}$$

where $f=c/(4\cdot h)$ is the fundamental frequency of natural vibrations of the reservoir (Newmark and Rosenblueth 1971).

Resultant Hydrodynamic Overturning Moment

The resultant earthquake hydrodynamic overturning moment on the base of the dam $M^0(t)$ is obtained by integrating along the height of the reservoir the forces exerted by the pressure field factored by their corresponding lever arms with respect to the base, i.e.

$$M^o(t) = h^2\cdot\int_0^1\zeta\cdot p^o(\zeta,t)d\zeta \tag{42}$$

Inserting Eq. (37) into Eq. (42) and recognizing that

$$\int_0^1\zeta\cdot\cos(\eta_m\cdot\zeta)d\varsigma = \frac{2}{(2\cdot m+1)\cdot\pi}\cdot\left((-1)^m-\frac{2}{(2\cdot m+1)\cdot\pi}\right) \tag{43a}$$

and

$$\int_0^1\zeta\cdot\sin(\eta_m\cdot\zeta)d\zeta = (-1)^m\cdot\left(\frac{2}{(2\cdot m+1)\cdot\pi}\right)^2 \tag{43b}$$

the resultant hydrodynamic overturning moment on the dam base is obtained as

$$M^o(t) = 16\cdot\frac{w_o\cdot c\cdot\gamma\cdot h^2}{\pi^3}\cdot\sum_{m=0}^{\infty}\frac{(-1)^m}{(2\cdot m+1)^3}\cdot\left\{-A_{0m}(t)\cdot(1-(-1)^m\cdot\eta_m)-\frac{1}{\alpha}\cdot(-1)^m\cdot A_{1m}(t)\right\} \tag{44a}$$

or, normalizing, for a nondimensional solution, Eq. (44*a*) may be written as

$$\Xi_0 = \frac{M^o(t)}{w_o\cdot h^3} = \frac{64}{\pi^3}\cdot\gamma\cdot f\cdot\sum_{m=0}^{\infty}\frac{1}{(2\cdot m+1)^3}\cdot\left\{A_{0m}(t)\cdot[(-1)^{m+1}+\eta_m]-\frac{1}{\alpha}\cdot A_{1m}(t)\right\} \tag{44b}$$

Case Study

A simple case study provides insight into the influence of the foundation impedance ratio with respect to water (α) on the response of rigid dams to horizontal ground motion acceleration. During this study, three extreme values of α (0.1, 1.0, 1e+6) were considered to emphasize the effect of including the elasticity of the sub-bottom materials in the model. The first value (α=0.1) represents a "highly gaseous" sub-bottom. These are hypothetical materials with a large volumetric content of undissolved gases or any other components that constitute a phase with substantial less-than-water impedance. The second value (α=1) represents a

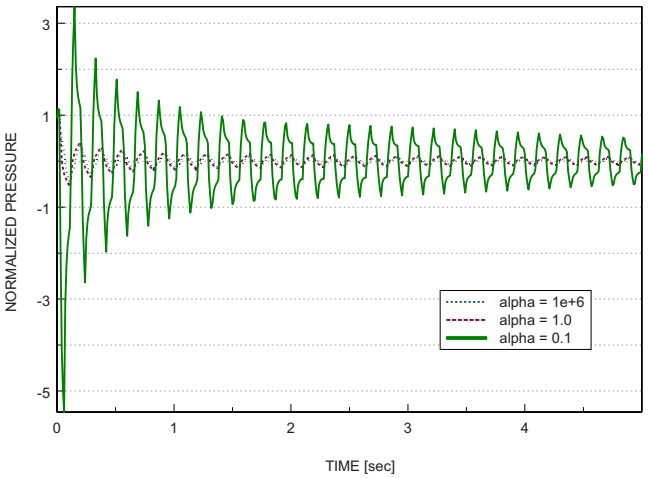

Fig. 3. Unit-impulse response function for the reservoir hydrodynamic pressure on the vertical face of a rigid dam facing a headwater height of $h=65$ m, at a nondimensional height of $\zeta=0.40$, for several values of the bottom impedance ratio α

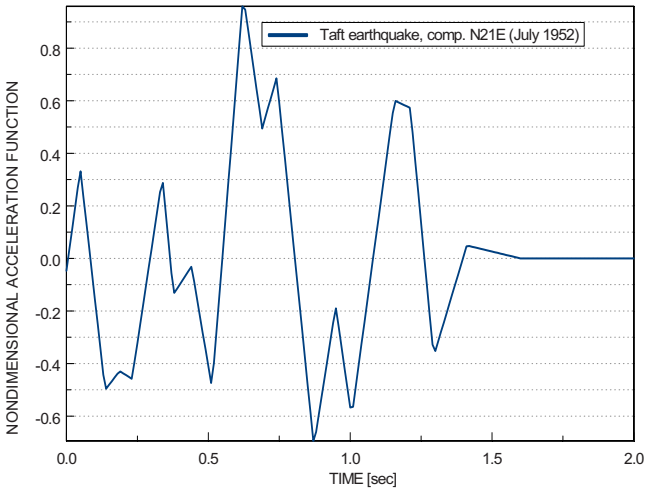

Fig. 4. Input ground motion accelerogram: Taft earthquake, N21E component (July 1952), as recorded and base-corrected in the interval $t\in[6.014, 7.425]$ s. Peak ground acceleration (PGA)=0.1601 g (Input accelerogram segment was extended with zero values for a total duration of 2.0 s).

type of reservoir bottom that is just an extension of the water medium down toward infinity. Liquefied reservoir bottoms with solid particles in suspension would have α values in the upper vicinity of $\alpha=1$. The last value ($\alpha=1e+6$) represents a very rigid sub-bottom, as in models that do not include interaction with the sub-bottom materials.

Fig. 3 shows the normalized unit-impulse response function for the reservoir hydrodynamic pressure on the vertical face of a rigid dam facing a headwater height of $h=65$ m, at a nondimensional height of $\zeta=0.40$, for the three extreme values of α. The function $F^o(\zeta,t)/(\rho\cdot c)$ is given by Eq. (35*a*). Notice the effect of including the parameter α in the formulation. At this scale, the plot does not show much difference between the functions for a rigid and for elastic solid sub-bottoms. But the function is dramatically magnified for highly gaseous sub-bottom materials. This extreme contrast is indicative of hydrodynamic-force amplifications when α is smaller than 1 (more and more so as α decreases toward its lower bound, zero), particularly, if the input ground motion accelerogram contains large pulses.

Fig. 4 shows the input accelerogram selected in the study. This is a short-duration (slightly less than 2 s) segment of the recorded and base-corrected N21E component of the Taft earthquake (July 1952). The peak ground acceleration is only 0.16*g*, but the record contains a large pulse of input energy.

Fig. 5(a) shows the normalized base shear-force response of a rigid dam facing a headwater height of $h=65$ m, when subjected to the selected input earthquake, for the three extreme values of α. The function Ω_o is given by Eq. (41*b*). As expected, the hydrodynamic force response is dramatically magnified for the highly gaseous sub-bottom materials.

To appreciate the effect of including the α parameter for solid-elastic sub-bottoms in the reservoir model, the functions for $\alpha=1e+6$ (rigid sub-bottom materials) and $\alpha=1$ (water extension) are plotted again (at the appropriate scale) in Fig. 5(b). Notice that, generally, there is an attenuation of force response when the elasticity of the reservoir foundation is included in the model. The parameter α clearly provides the system with an effective energy dissipating mechanism (radiation damping) for this particular earthquake accelerogram.

Similar conclusions are derived for the overturning moment response at the base of the dam, as shown in Fig. 6, where the nondimensional function Ξ_o, given by Eq. (44*b*), has been plotted.

Response Spectra

The maximum absolute values of the results provided by Eqs. (41*b*) and (44*b*) during the history of response for a specific input earthquake may be used to construct a family of seismic response spectra for base shear force and overturning moment, respectively, useful for dam analysis and design. The independent abscissa in the plot is the reservoir height, and the parameter identifying each spectrum in the family is the impedance ratio of the sub-bottom materials with respect to water. The ordinates represent the extreme values of Ω_o and Ξ_o for the normalized base shear force and overturning moment, respectively. For example, Figs. 7 and 8 compare these spectra for a rigid dam when subjected to the selected portion of the Taft earthquake accelerogram, N21E component (July 1952), for a very stiff reservoir bottom ($\alpha=1e+6$) and for a highly gaseous reservoir bottom ($\alpha=0.1$). As expected, the hydrodynamic forces are much larger for the reservoir foundation with $\alpha=0.1$ than for the rigid sub-bottom case.

Figs. 9 and 10 show the comparison for the same parameters of response, but this time between the spectra for the case of a rigid sub-bottom and the case for an "extended water" at the reservoir base. The results suggest a substantial attenuation of the earthquake-induced hydrodynamic forces (by a factor of 1/4 to 1/2) for reservoir heights larger than about 45 m and amplification of the base shear force for reservoir heights smaller than about 30 m, for the specific selected earthquake, and when the elasticity of the solid sub-bottom materials is included in the model, as compared to those forces for a rigid reservoir foundation.

Conclusions

In this investigation, a two-dimensional time-domain closed-form mathematical model for the hydrodynamic forces on the upstream

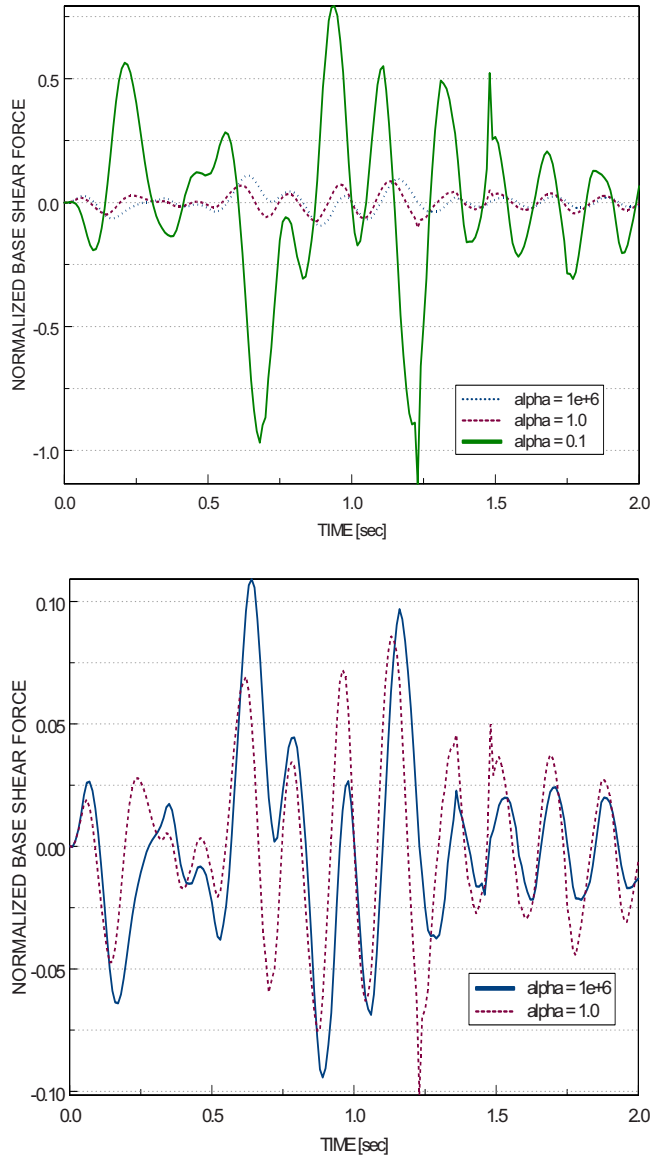

Fig. 5. (a) Base shear-force response of a rigid dam facing a headwater height of $h=65$ m, when subjected to the selected portion of the Taft earthquake accelerogram, N21E component (July 1952), for several values of the reservoir bottom impedance ratio α; (b) contrasting two of the base shear-force responses in (a): for a very stiff reservoir bottom ($\alpha=1e+6$) versus the same response for an almost-water reservoir bottom ($\alpha=1.0$)

vertical face of a given rigid dam under a specified horizontal ground motion accelerogram was developed. The model includes the absorption of energy at the elastic reservoir bottom, which is characterized by the impedance ratio of the sub-bottom materials with respect to water.

The assumption of a rigid, i.e., nonabsorptive, reservoir boundary may lead to an overestimation of the earthquake response of the dam-reservoir-foundation system. In particular, the effective lateral load on the upstream face of an existing concrete gravity dam may be overestimated and the associated recommended retrofit expenditures unnecessary. This was proved true in this investigation for reservoir heights exceeding about 45 m when subjected to the selected input earthquake accelerogram. By contrast, there was base shear force amplification for reservoir heights smaller than about 30 m, when the elastic sub-bottom was

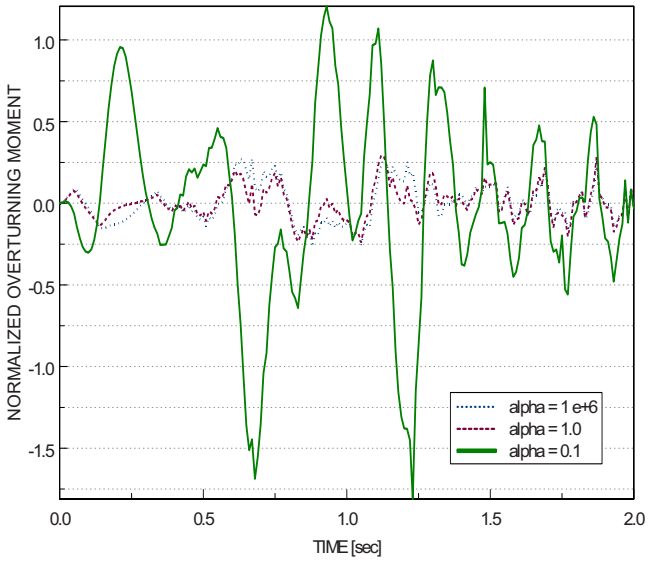

Fig. 6. Overturning moment at the base of a rigid dam facing a headwater height of $h=65$ m when subjected to the selected portion of the Taft earthquake accelerogram, N21E component (July 1952), for several values of the reservoir bottom impedance ratio α

included in the model, as compared with the results for rigid sub-bottom.

On the other hand, a reservoir with sub-bottom materials with less-than-water impedance is expected to exert earthquake-induced forces on a rigid barrier larger than those in the case of a rigid reservoir sub-bottom. This force amplification grows with decreasing values of the impedance ratio of the sub-bottom materials with respect to water, α, in the range between 0 and 1.

The assessment of the impedance ratio of the sub-bottom materials relative to water (α) remains a difficult task. For one, this parameter varies spatially across the bottom of the impounded water, by virtue of the irregularity of the foundation layers. And

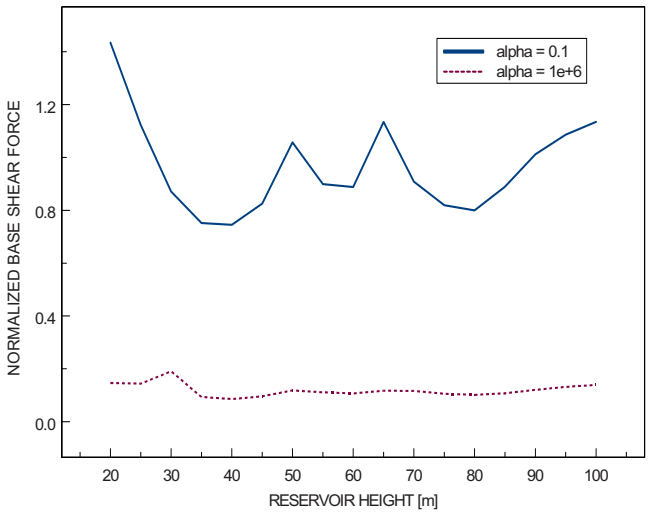

Fig. 7. Response spectra for the shear force at the base of a rigid dam when subjected to the selected portion of the Taft earthquake accelerogram, N21E component (July 1952), for a very stiff reservoir bottom ($\alpha=1e+6$) and for a 'highly gaseous' reservoir bottom ($\alpha=0.1$)

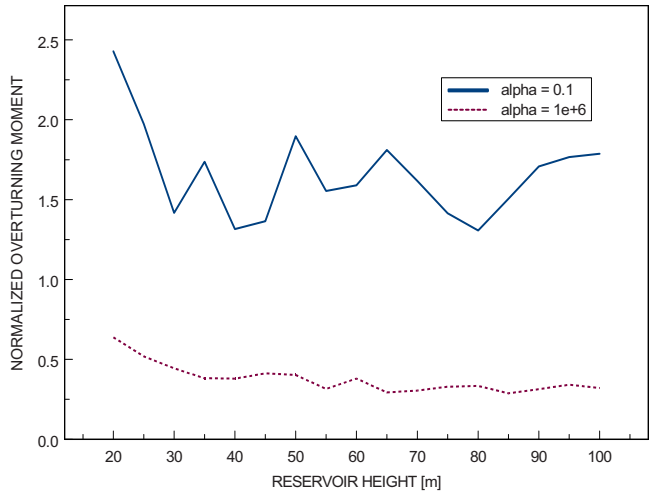

Fig. 8. Response spectra for the overturning moment at the base of a rigid dam when subjected to the selected portion of the Taft earthquake accelerogram, N21E component (July 1952), for a very stiff reservoir bottom ($\alpha = 1e+6$) and for a highly gaseous reservoir bottom ($\alpha = 0.1$)

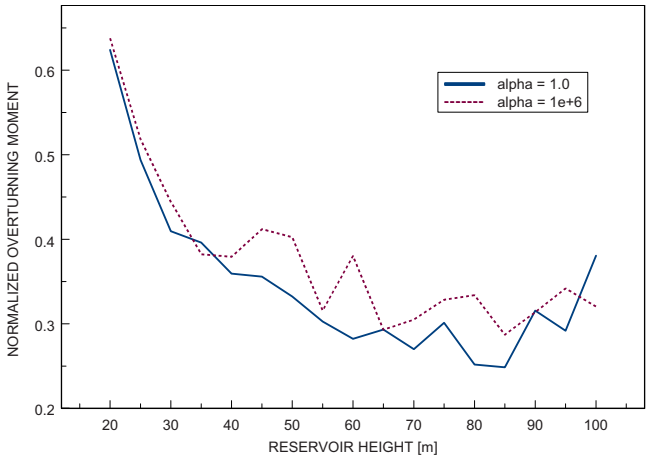

Fig. 10. Response spectra for the overturning moment at the base of a rigid dam when subjected to the selected portion of the Taft earthquake accelerogram, N21E component (July 1952), for a very stiff reservoir bottom ($\alpha = 1e+6$) and for an almost water reservoir bottom ($\alpha = 1.0$)

for another, the probing mechanism must be able to penetrate the bottom to a sufficient depth as to provide samples representative of the various substrata.

During the last two decades, several investigators have conducted projects in the field attempting to quantify the parameter α in real reservoir-dam situations. The underlying experiments were based on seismic analyses of reflected and refracted pressure-wave signals generated with small explosives (Ghanaat and Redpath 1995) or on the scattering of sonar-acoustics emissions (McGee et al. 1995). The objective of these waterborne seismic scattering surveys was to estimate an average value of α for a dam location and the associated dispersion, represented by a coefficient of variation. In a project targeting seven specific concrete dams in the U.S. (Ghanaat and Redpath 1995), the average value of α was inferred in the range of 0.3–5.0, with a coefficient of variation of about 0.25, with results strongly dependent on the actual amount of sediments deposited in the area close to the upstream face of the nonoverflow monoliths of the dams.

Notice that, generally, the effective impedance ratio of the sub-bottom materials is sensitive to the specific type of input earthquake. Upon earthquake-induced oscillations with reversal of loading, the initial stiffness of the sub-bottom materials may deteriorate, thereby modifying the effective elasticity of the underlying strata and their associated α-value. Much more research is needed to evaluate the variation of response spectra for design parameters of response with the characteristics of the input ground motion for a given reservoir-dam-foundation site.

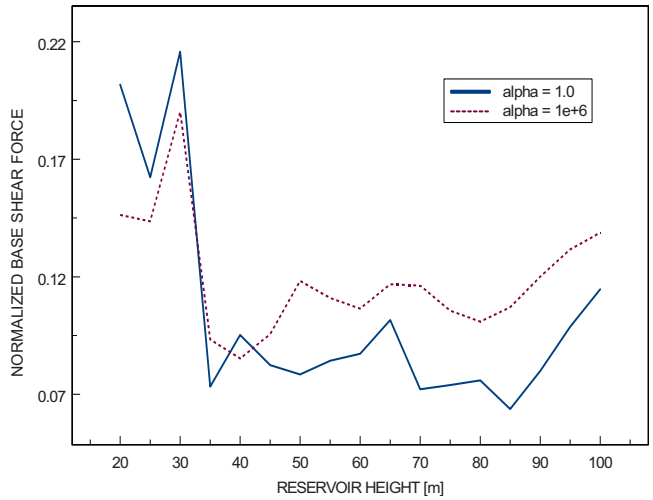

Fig. 9. Response spectra for the shear force at the base of a rigid dam when subjected to the selected portion of the Taft earthquake accelerogram, N21E component (July 1952), for a very stiff reservoir bottom ($\alpha = 1e+6$) and for an 'almost-water' reservoir bottom ($\alpha = 1.0$)

Acknowledgments

This investigation was conducted under the Work Unit "Nonlinear Behavior and Failure Mechanisms of Concrete Dams (Foundation and Bottom Absorption)," of the Earthquake Engineering Research Program, part of the Research Program on Civil Works sponsored by the Department of the Army, Corps of Engineers, Headquarters. The writers gratefully acknowledges the support and guidance provided by the Office of the Chief of Engineers and by the Army Engineer District representatives in the Field Review Group. Approved for public release; distribution is unlimited. Permission to publish was granted by the Director of the Geotechnical and Structures Laboratory, U.S. Army Engineer Research and Development Center.

References

Bouaanani, N., Paultre, P., and Proulx, J. (2003). "A closed-form formulation for earthquake-induced hydrodynamic pressure on gravity dams." *J. Sound Vib.*, 261, 573–582.

Bougacha, S., and Tassoulas, J. L. (1991). "Seismic response of gravity dams. II: Effects of sediments." *J. Eng. Mech.*, 117(8), 1839–1850.

Bowman, F. (1958). *Introduction to Bessel functions*, Dover, New York.

Cheng, A. H.-D. (1986). "Effect of sediment on earthquake-induced reservoir hydrodynamic response." *J. Eng. Mech.*, 112(7), 654–665.

Clough, R. W., and Penzien, J. (1993). *Dynamics of structures*, McGraw-Hill, New York.

Fenves, G., and Chopra, A. K. (1983). "Effects of reservoir bottom absorption on earthquake response of concrete gravity dams." *Earthquake Eng. Struct. Dyn.*, 11(6), 809–829.

Fenves, G., and Chopra, A. K. (1984a). "Earthquake analysis of concrete gravity dams including reservoir bottom absorption and dam-water-foundation rock interaction." *Earthquake Eng. Struct. Dyn.*, 12(5), 663–680.

Fenves, G., and Chopra, A. K. (1984b). "Earthquake analysis and response of concrete gravity dams." *Rep. No. UCB/EERC-84/10*, Univ. of California/Earthquake Engineering Research Center, Berkeley, Calif.

Fenves, G., and Chopra, A. K. (1985a). "Effects of reservoir bottom absorption and dam-water-foundation rock interaction on frequency response functions for concrete gravity dams." *Earthquake Eng. Struct. Dyn.*, 13(1), 13–31.

Fenves, G., and Chopra, A. K. (1985b). "Reservoir bottom absorption effects in earthquake response of concrete gravity dams." *J. Struct. Eng.*, 111(3), 545–562.

Ghanaat, Y., and Redpath, B. B. (1995). "Measurements of reservoir-bottom reflection coefficient at seven concrete dam sites." *Rep. No. QS95-01*, Bureau of Reclamation, Denver, Colo., and the Dept. of the Army, Waterways Experiment Station, Corps of Engineers, Vicksburg, Miss.

Gogoi, I., and Maity, D. (2006). "A non-reflecting boundary condition for the finite element modeling of infinite reservoir with layered sediment." *Adv. Water Resour.*, 29, 1515–1527.

Hall, J. F., and Chopra, A. K. (1982). "Two-dimensional dynamic analysis of concrete gravity and embankment dams including hydrodynamic effects." *Earthquake Eng. Struct. Dyn.*, 10(2), 305–332.

Kotsubo, S. (1959). "Dynamic water pressure on dams due to irregular earthquakes." *Mem. Fac. Eng., Kyushu Univ.*, 18(4), 119–129.

McGee, R. G., Ballard, R. F., and Caulfield, D. D. (1995). "A technique to assess the characteristics of bottom and sub-bottom marine sediments." *Technical Rep. No. DRP-95-3*, Dept. of the Army, Waterways Experiment Station, Corps of Engineers, Vicksburg, Miss.

Newmark, N. M., and Rosenblueth, E. (1971). *Fundamentals of earthquake engineering*, Prentice-Hall, Englewood Cliffs, N.J.

Rosenblueth, E. (1968). "Presión hidrodinámica en presas debida a la aceleración vertical con refracción en el fondo." *II Congreso Nacional de Ingeniería Sísmica*, Instituto de Ingeniería, Veracruz, Mexico.

Weber, B. (1994). "Rational transmitting boundaries for time-domain analysis of dam-reservoir interaction." Doctor of Technical Science dissertation, Swiss Federal Institute of Technology, Zurich, Switzerland.

Wylie, C. R. (1975). *Advanced engineering mathematics*, McGraw-Hill, New York, NY.

Zwillinger, D. (1996). *Standard mathematical tables and formulae*, 30th Ed., CRC Press, Boca Raton, Fla.